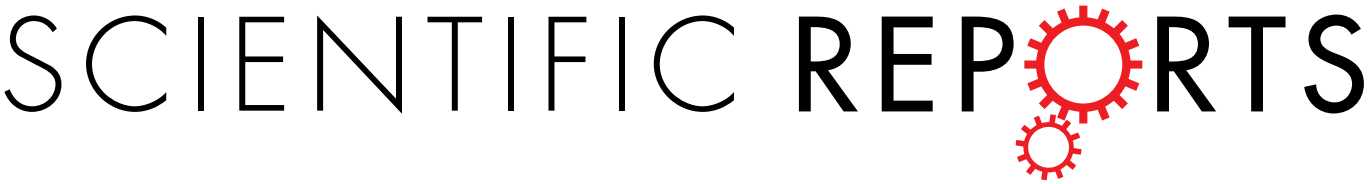

OPEN

Universal linear-temperature resistivity: possible quantum diffusion transport in strongly correlated superconductors

Received: 19 April 2017
Accepted: 28 July 2017
Published online: 25 August 2017

Tao Hu[1,2], Yinshang Liu[1,2], Hong Xiao[3], Gang Mu[1,2] & Yi-feng Yang[4,5,6]

The strongly correlated electron fluids in high temperature cuprate superconductors demonstrate an anomalous linear temperature (*T*) dependent resistivity behavior, which persists to a wide temperature range without exhibiting saturation. As cooling down, those electron fluids lose the resistivity and condense into the superfluid. However, the origin of the linear-*T* resistivity behavior and its relationship to the strongly correlated superconductivity remain a mystery. Here we report a universal relation $d\rho/dT = (\mu_0 k_B/\hbar)\lambda_L^2$, which bridges the slope of the linear-*T*-dependent resistivity ($d\rho/dT$) to the London penetration depth λ_L at zero temperature among cuprate superconductor $Bi_2Sr_2CaCu_2O_{8+\delta}$ and heavy fermion superconductors $CeCoIn_5$, where μ_0 is vacuum permeability, k_B is the Boltzmann constant and $\hbar$ is the reduced Planck constant. We extend this scaling relation to different systems and found that it holds for other cuprate, pnictide and heavy fermion superconductors as well, regardless of the significant differences in the strength of electronic correlations, transport directions, and doping levels. Our analysis suggests that the scaling relation in strongly correlated superconductors could be described as a hydrodynamic diffusive transport, with the diffusion coefficient (*D*) approaching the quantum limit $D \sim \hbar/m^*$, where m^* is the quasi-particle effective mass.

In quantum mechanics, the uncertainty principle gives rise to quantum fluctuations of the system that may impose some universal bound on its physical properties. Calculations based on the AdS/CFT (Anti de-Sitter/Conformal Field Theory) have suggested a lower bound for the liquid viscosity, $\eta/s \geq \hbar/4\pi k_B$[1], where η is the shear viscosity and s the entropy. Recent experiments also revealed a quantum bound $D_s \geq \hbar/m$ for the spin diffusivity D_s in a strongly interacting Fermi gas[2,3]. Here $\hbar$ is the reduced Planck constant and m is the mass of particles. It is therefore interesting to ask if such a lower bound may be realized in the electron transport of strongly correlated quantum critical systems.

One of the distinguished features of strongly correlated cuprate superconductors is the linear-temperature (T) dependent resistivity[4], which could extend to very high temperature[4] and violate the Mott-Ioffe-Regel (MIR) limit[5]. The linear relationship has also been observed in some heavy fermion superconductors[6,7], starting at around the superconducting transition temperature T_c and extending to high temperatures of about 10–20 times of T_c. Many different mechanisms have been proposed to explain the microscopic origin of the linear-T resistivity behavior including quantum critical theories and the more exotic AdS/CFT calculations. On the other hand, recent experiment suggested that the linear-T resistivity in different materials may share a similar scattering rate[8].

In the present work, we investigated the linear-T resistivity in a number of strongly correlated superconductors and demonstrate a connection between its coefficient and the superfluid density responsible for the charge carrying in the superconducting state. We show that this can be understood by a diffusion transport of heavy

[1]State Key Laboratory of Functional Materials for Informatics, Shanghai Institute of Microsystem and Information Technology, Chinese Academy of Sciences, 865 Changning Road, Shanghai, 200050, China. [2]CAS Center for Excellence in Superconducting Electronics(CENSE), Shanghai, 200050, China. [3]Center for High Pressure Science and Technology Advanced Research, Beijing, 100094, China. [4]Beijing National Laboratory for Condensed Matter Physics and Institute of Physics, Chinese Academy of Sciences, Beijing, 100190, China. [5]Collaborative Innovation Center of Quantum Matter, Beijing, 100190, China. [6]School of Physical Sciences, University of Chinese Academy of Sciences, Beijing, 100190, China. Correspondence and requests for materials should be addressed to T.H. (email: thu@mail.sim.ac.cn) or H.X. (email: hong.xiao@hpstar.ac.cn)

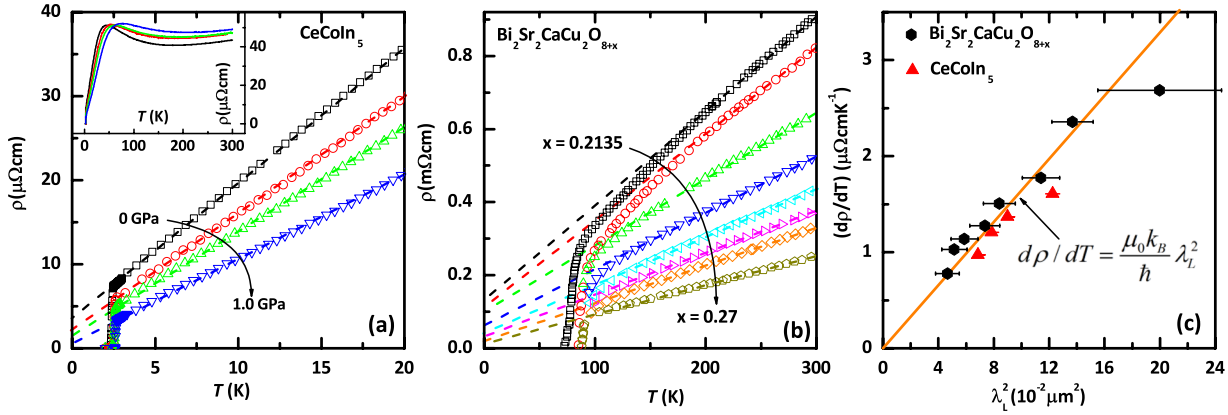

Figure 1. (**a**) T dependent resistivity ρ of $CeCoIn_5$ under the pressure 0, 0.3, 0.55, 1.0 GPa. The arrow points to the increase in pressures. Inset to 1(**a**) is the ρ of $CeCoIn_5$ up to 300 K. (**b**) T dependent resistivity ρ of oxygen doped $Bi_2Sr_2CaCu_2O_{8+x}$ with $x = 0.2135$, 0.217, 0.22, 0.24, 0.245, 0.255, 0.26, 0.27, respectively. The arrow points to the Bi2212 from underdoped to overdoped. The resistivity data of $Bi_2Sr_2CaCu_2O_{8+x}$ are taken from the literature[22]. (**c**) Linear scale plot of $d\rho/dT$ vs. λ_L^2 for $CeCoIn_5$ (red triangles) and $Bi_2Sr_2CaCu_2O_{8+x}$ (Bi2212) (black circles). $d\rho/dT$ is the slope of linear-temperature-dependent resistivity, and λ_L is the London penetration depth of superconductors at zero temperature. The straight line corresponds to $d\rho/dT = (\mu_0 k_B/\hbar)\lambda_L^2$, where ρ is in the unit of $\mu\Omega cm$, λ_L is in μm, and T is in K. See Table 1 for details, including errors.

quasi-particles whose diffusion coefficient approaches the quantum limit $D = \hbar/m^*$, where m^* is the effective mass of the quasi-particles.

Results

We start with the heavy fermion superconductor $CeCoIn_5$. Among all strongly correlated superconductors, $CeCoIn_5$ is remarkably similar to the high T_c cuprate superconductors in several aspects[9]. For example, it has also a two-dimensional Fermi surface[10,11], its superconducting phase is near to an antiferromagnetic phase[12–14], and its superconducting gap has d-wave symmetry[15–17]. Besides, $CeCoIn_5$ is one of the purest strongly correlated superconductors[6,7], with a tunable linear-T resistivity under modest applied pressure[18–21]. To examine its transport properties, we have therefore grown high quality $CeCoIn_5$ single crystal samples by an indium self-flux method[6] and performed detailed transport measurements under pressure to avoid disorder related effects.

Figure 1(a) demonstrates the T-dependent resistivity curve of $CeCoIn_5$ under pressure from 0 GPa to 1.0 GPa. All of them exhibit a perfect linear-in-T resistivity from around T_c to about 20 K as indicated by the dashed lines. The inset of Fig. 1(a) shows the T-dependent resistivity of $CeCoIn_5$ up to 300 K. For comparison, we also plot in Fig. 1(b) the resistivity of $Bi_2Sr_2CaCu_2O_{8+x}$ from underdoped to overdoped regime with the oxygen contents from $x = 0.2135$ to 0.27[22]. Figure 1(c) demonstrates the $d\rho/dT$ versus λ_L^2 for both compounds, using the experimental results for the penetration depth measured previously by muon spin spectroscopy[23] and ac susceptibility[24]. We see remarkably that all the investigated samples fall on the same straight line described by $d\rho/dT = (\mu_0 k_B/\hbar)\lambda_L^2$, with a coefficient that is determined entirely by the fundamental constants (μ_0: the vacuum permeability; k_B: the Boltzmann constant; $\hbar$: the reduced Planck constant). This indicates a universal origin for the charge transport in both compounds.

The above relation between $d\rho/dT$ and λ_L^2 can be extended to various other strongly correlated superconductors with linear-T resistivity. The data are summarized in Fig. 2 on a log-log scale. Most resistivity data were taken from experimental results on high-quality single crystal samples in order to obtain the intrinsic linear-in-T coefficient. The values of the penetration depth were obtained by muon spin spectroscopy[25], optical conductivity measurement[26,27] and some other techniques. Note that for superconducting thin films, the experimental magnetic penetration depth generally deviates from the London penetration depth λ_L due to structural disorders in the films[28,29]. Even in high quality ultrathin films, there is a large difference in superfluid density between the film and the bulk materials with same T_c[30,31]. Consequently all the data of the London penetration depth shown in Fig. 2 were taken only from bulk materials. It is worth noting that Fig. 2 also includes the transport data for cuprate superconductors along different transport directions, e.g., $YBa_2Cu_3O_{6.93}$ along the a, b and c-axis. Cuprates generally exhibit a metallic in-plane resistivity but an insulating-like resistivity along the c-axis below certain temperature, which reflects the two-dimensional nature of the system. Correspondingly, the penetration depth along the c-axis is determined by a Josephson-coupling between superconducting layers[32–34], which is different from the in-plane one[26]. Thus it is amazing to observe that the same scaling relation holds true for both directions. Combining the data for all the strongly correlated superconductors summarized here, we see that the scaling, $d\rho/dT = (\mu_0 k_B/\hbar)\lambda_L^2$, spans over several orders of magnitude. Note that the in-plane LSCO data in the extremely underdoped regime $0.07 \le p \le 0.12$ demonstrates a systematic deviation from the scaling relationship as shown in Fig. 2. The deviation could be understood in terms of the complex competing phase, like charge density wave and pseudogap, which become significant in the underdoped regime.

Material	label	T_c(K)	$d\rho/dT(\mu\Omega cmK^{-1})$	T-linear range in calculation (K)	Refs	$\lambda L(nm)$	Refs
c-axis$YBa_2Cu_3O_{6.93}$	1	92	12.3 ± 0.07	250–400		923	
c-axis$YBa_2Cu_3O_{6.88}$	2	92	12.8 ± 0.17	300–400		1400	26
c-axis$YBa_2Cu_3O_{6.78}$	3	82	30 ± 0.84	320–400	49	2900	
a-axis $YB_2Cu_3O_{6.93}$	$YBa_2Cu_3O_x$	92	0.78 ± 0.001	105–300		160	
b-axis$YBa_2Cu_3O_{6.93}$			0.37 ± 0.004	150–300		100	50, 51
a-axis $YB_2Cu_3O_7$			0.95 ± 0.002	110–300	52	160	
b-axis$YBa_2Cu_3O_7$			0.43 ± 0.003	255–300		100	
$Tl_2Ba_2CuO_{6+x}$	$Tl_2Ba_2CuO_{6+x}$	80	1.55 ± 0.001	120–300	53	240 ± 20	54
c-axis $Tl_2Ba_2CuO_{6+x}$		85	2681 ± 3.4	220–300	55	17500 ± 2500	55–57
$Bi_2Sr_2CaCu_2O_{8+x}$ ($x = 0.2135$)	$Bi_2Sr_2CaCu_2O_{8+x}$	72 ± 2	2.68 ± 0.01	200–300		447 ± 50	
$Bi_2Sr_2CaCu_2O_{8+x}$ ($x = 0.217$)		79.3	2.36 ± 0.02	200–300		370 ± 20	
$Bi_2Sr_2CaCu_2O_{8+x}$ ($x = 0.22$)		81.9	1.78 ± 0.003	180–300		338 ± 20	
$Bi_2Sr_2CaCu_2O_{8+x}$ ($x = 0.24$)		87.9	1.5 ± 0.002	160–300		290 ± 20	
$Bi_2Sr_2CaCu_2O_{8+x}$ ($x = 0.245$)		89	1.28 ± 0.002	155–300	22, 58	271 ± 20	24
$Bi_2Sr_2CaCu_2O_{8+x}$ ($x = 0.255$)		87.8	1.14 ± 0.001	150–300		243 ± 20	
$Bi_2Sr_2CaCu_2O_{8+x}$ ($x = 0.26$)		86	1.03 ± 0.001	125–300		227 ± 20	
$Bi_2Sr_2CaCu_2O_{8+x}$ ($x = 0.27$)		84	0.78 ± 0.01	105–300		216 ± 20	
$SrFe_2(As_{0.7}P_{0.3})_2$	$SrFe_2(As_{0.7}P_{0.3})_2$	25	0.7 ± 0.01	100–300	59	270 ± 10	59
$BaFe_2(As_{0.67}P_{0.33})_2$	$BaFe_2(As_{0.67}P_{0.33})_2$	29.5	1.16 ± 0.001	31–150	60	315 ± 15	61
$NaFe_{0.97}Co_{0.03}As$	$NaFe_{0.97}Co_{0.03}As$	21.8	1.46 ± 0.004	50–250	62	375 ± 15	62
FeSe	FeSe	8	5.84 ± 0.01	20–80	63	425 ± 20	64
c-axis $La_{1.9}Sr_{0.1}CuO_4$	4	27	160 ± 0.5	500–800		5908 ± 400	
c-axis $La_{1.9}Sr_{0.12}CuO_4$	3	30	195 ± 0.2	300–800	65	5345 ± 400	
c-axis $La_{1.88}Sr_{0.15}CuO_4$	2	35.8	154.8 ± 0.3	300–800		3816 ± 280	
c-axis $La_{1.8}Sr_{0.2}CuO_4$	1	31.7	147.6 ± 0.2	320–800		2441 ± 200	
$La_{1.85}Sr_{0.15}CuO_4$	$La_{2-x}Sr_xCuO_4$ - Hussey		1.7 ± 0.4	The slope are directly taken from Hussey *et al.*[67],		249 ± 20	
$La_{1.84}Sr_{0.16}CuO_4$			1.5 ± 0.4			229 ± 20	
$La_{1.83}Sr_{0.17}CuO_4$			1.4 ± 0.4			213 ± 20	
$La_{1.82}Sr_{0.18}CuO_4$			1.2 ± 0.4			203 ± 15	
$La_{1.81}Sr_{0.19}CuO_4$			1.1 ± 0.4			198 ± 15	
$La_{1.8}Sr_{0.2}CuO_4$			1.1 ± 0.4			197 ± 15	
$La_{1.79}Sr_{0.21}CuO_4$			1.05 ± 0.4			198 ± 15	
$La_{1.78}Sr_{0.22}CuO_4$			0.9 ± 0.4			199 ± 15	
$La_{1.77}Sr_{0.23}CuO_4$			1.08 ± 0.4			199 ± 15	
$La_{1.76}Sr_{0.24}CuO_4$			1.0 ± 0.4			199 ± 15	
$La_{1.93}Sr_{0.07}CuO_4$	$La_{2-x}Sr_xCuO_4$	12.3	4.79 ± 0.018	200–400		497 ± 37	66
$La_{1.92}Sr_{0.08}CuO_4$		22	3.96 ± 0.016	200–400		377 ± 30	
$La_{1.91}Sr_{0.09}CuO_4$		24.5	3.21 ± 0.02	200–400		314 ± 30	
$La_{1.9}Sr_{0.1}CuO_4$		27.5	2.75 ± 0.003	250–400		286 ± 30	
$La_{1.89}Sr_{0.11}CuO_4$		29.6	2.34 ± 0.002	250–400		282 ± 30	
$La_{1.88}Sr_{0.12}CuO_4$		30.4	2.05 ± 0.002	250–400		280 ± 20	
$La_{1.87}Sr_{0.13}CuO_4$		34.6	1.72 ± 0.001	200–400		277 ± 20	
$La_{1.86}Sr_{0.14}CuO_4$		36.3	1.54 ± 0.006	200–400		268 ± 20	
$La_{1.85}Sr_{0.15}CuO_4$		39.3	1.44 ± 0.001	180–400		249 ± 20	
$La_{1.84}Sr_{0.16}CuO_4$		36.6	1.26 ± 0.004	130–400	68	229 ± 20	
$La_{1.83}Sr_{0.17}CuO_4$		35.7	1.18 ± 0.004	200–400		213 ± 20	
$La_{1.82}Sr_{0.18}CuO_4$		36	1.05 ± 0.003	200–400		203 ± 15	
$La_{1.81}Sr_{0.19}CuO_4$		33	0.99 ± 0.006	50–400		198 ± 15	
$La_{1.8}Sr_{0.2}CuO_4$		30.3	0.96 ± 0.001	150–400		197 ± 15	
$La_{1.79}Sr_{0.21}CuO_4$		28.5	0.92 ± 0.001	220–400		198 ± 15	
$La_{1.78}Sr_{0.22}CuO_4$		25.5	0.88 ± 0.001	260–400		199 ± 15	
$Bi_2Sr_{1.8}La_{0.2}CuO_{6+\delta}$	$Bi_2Sr_{2-x}La_xCuO_{6+\delta}$	28.1	1.24 ± 0.004	250–300		319 ± 25	
$Bi_2Sr_{1.6}La_{0.4}CuO_{6+\delta}$		29	1.62 ± 0.004	250–300		297 ± 20	69
$Bi_2Sr_{1.4}La_{0.6}CuO_{6+\delta}$		12	3.25 ± 0.01	250–300		553 ± 40	
UPt_3	UPt_3	0.5	9.2 ± 0.2	5–10	70	715	70
c-axis Upt_3		0.5	3.3 ± 0.12	5–10		422	
$CeCoIn_5$ (0 Gpa)	$CeCoIn_5$	2.3	1.61 ± 0.008	3–20		350 ± 12	
$CeCoIn_5$ (0.3 Gpa)		2.51	1.36 ± 0.007	3–20		300 ± 12	
$CeCoIn_5$ (0.55 Gpa)		2.58	1.20 ± 0.002	3–20	Our data	280 ± 12	23
$CeCoIn_5$ (1 Gpa)		2.63	0.97 ± 0.004	3–20		262 ± 12	

Table 1. Transport parameters and London penetration depth at zero temperature.

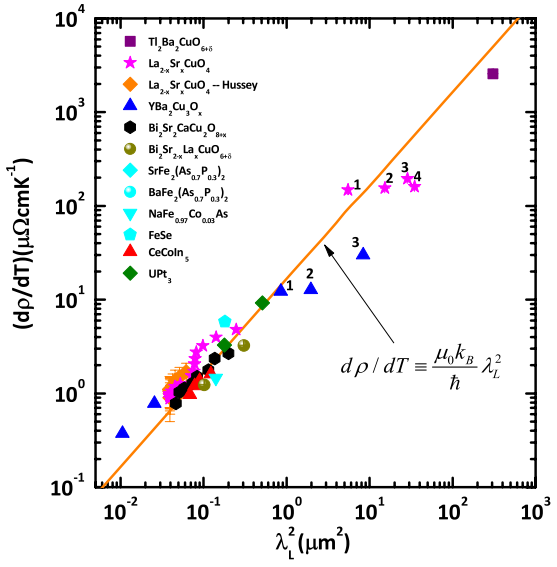

Figure 2. Log-log plot of $d\rho/dT$ vs. λ_L^2 for various strongly correlated superconductors. The orange line is the scaling relation $d\rho/dT = (\mu_0 k_B/\hbar)\lambda_L^2$. See Table 1 for details, including errors.

The above scaling relation is consistent with several well-known experimental facts. First, considering the special case at $T = T_c$ and neglecting the residual resistivity, the scaling relation $d\rho/dT \propto \lambda_L^2$ gives the well-known Homes's law, $\sigma_c T_c \propto \lambda_L^{-2}$, where σ_c is the *dc* conductivity at T_c[26]. Second, the Drude formula[35] is often used to describe the resistivity of conventional metals, $\rho = m^*/n_n e^2\tau$, where m^* is the effective mass of the quasi-particles, n_n is the carrier density of quasi-particles, e is the charge of electrons, and τ is the relaxation time. If we naively match the Drude formula with the above scaling relation for a non-quasiparticle system and assume that the normal fluid and the superfluid are composed of the same charge carriers, $\lambda_L = (m^*/\mu_0 n_n e^2)^{1/2}$, we obtain immediately a material-independent scattering rate $\tau^{-1} = k_B T/\hbar$ for all these strongly correlated superconductors. This is consistent with the universal scattering rate recently observed in the linear-in-T resistivity region among good and "bad" metals[8]. However, one can not take it for granted that the normal fluid in Drude model and superfluid in London equation are always the same. Actually, experiments showed that only part of normal carriers condensate into superfluid[36]. In addition, the measurements of the London moment already revealed the mass of Cooper pairs are undressed and have twice of the electron's bare mass, regardless the conventional metal superconductors[37], heavy fermion superconductors[38] or cuprates[39], which is different from the effective mass in the Drude formula. These results suggest that the mass and carrier density of the superfluid (n_s) and the normal fluid (n_n) are different in strongly correlated superconductors. So one can not directly obtain the universal scaling relation simply by replacing ρ with Drude model and λ_L with London equation. The universal scaling relation $d\rho/dT = (\mu_0 k_B/\hbar)\lambda_L^2$ has much deeper physics, which directly links the superfluid at zero temperature to the normal fluid responsible for the linear-in-T resistivity in strongly correlated superconductors. It reveals an underlying relation between the superfluid and normal carriers: $n_s/m_e = n_n/m^*$. And indeed experimental evidence shows that about one of fourth normal carriers[36] condensates into superfluid in optimal doped cuprates while the effective mass of optimum cuprates is about 3–4 times of the electron free mass[36,40], which validate $n_s/m_e = n_n/m^*$.

The above result provides important information on the nature of the electron transport in the quantum critical regime. Recently, several experiments have shown that electrons in solid can exhibit hydrodynamic flows similar to a classical viscous liquid, if the electron fluid equilibrates by the electron-electron collisions[41–43]. Thus the electron transport in strongly correlated superconductors, where electron-electron interactions play a major role in the scattering processes, might in principle have a hydrodynamic description. Consequently, its linear-in-T resistivity could be described by the well-known Einstein's relation[44], an important law for the hydrodynamic transport, which states that the mobility (μ) of a particle in a fluid is related to its diffusion coefficient (D), namely, $D = \mu k_B T$. Hence we have $\rho = k_B T/n_n e^2 D$ and in the linear-in-T regime, the diffusion coefficient D must be a temperature-independent constant. Combining this and the scaling relation immediately yields $D = \hbar/m^*$, which is the quantum limit of the charge diffusion coefficient for the quasi-particles with an effective mass, m^*. This is one of the most important consequence of our observations. Actually, the quantum limit of the diffusion coefficient was recently observed in cold fermionic atomic gases in the unitary limit of scattering[2,3]. It implies that quantum diffusion transport might be a universal property of strongly correlated fermionic systems where the electron scatterings are so strong that the transport becomes highly incoherent. In fact, it was proposed recently that the transport in an incoherent metal is controlled by the collective diffusion of energy and charge[45], supporting the proposed scenario of quantum diffusion transport in the present work. Thus, the obtained scaling relation suggests the superfluid could also be governed by the quantum diffusion, since it connects the ground state with the normal state in the strongly correlated superconductors.

Our results also provide some insights on the nature of strongly correlated superconductivity, which is often born out of strongly correlated normal fluid in the quantum critical regime. Since the latter already approaches

the quantum diffusion limit before it transits into the superfluid state, it implies a zero-point motion of the superfluid. Some people considered the quantum diffusion as a necessary condition for the presence of superfluid[46,47]. In fact, the quantum diffusion might explain the Uemura results for superconducting transition temperatures. Y. Uemura *et al*. observed that the underdoped cuprate superconductors exhibit a Bose-Einstein-condensation (BEC)-like superconducting transition but with a reduced transition temperature[25,48]. Actually, the BEC generally occurs when the thermal de Broglie wavelength λ_{dB} is comparable to the distance between bosons, where λ_{dB} characterizes a length scale within which the bosons can be regarded as quantum mechanical wave-packets. However, the quantum diffusion gives a new length scale $\xi_{Th} = \sqrt{D\tau}$ with $\tau = \hbar/k_BT$, which characterizes the length scale that carriers can travel before losing their quantum coherence. Since the diffusion length $\xi_{Th} = \sqrt{\hbar^2/m^*k_BT}$ is less than $\lambda_{dB} = \sqrt{2\pi\hbar^2/2m^*k_BT}$ of electron pairs under certain temperature, it makes ξ_{Th} a new dephasing length to determine the *BEC* temperature. Thus the BEC temperature (T_B) is reduced to $T_c/T_B = (\xi_{Th}/\lambda_{dB})^2 = 1/\pi$ as observed in the Uemura plot[25,48].

Conclusion

In summary, we observed a universal scaling relation $d\rho/dT = (\mu_0 k_B/\hbar)\,\lambda_L^2$, which connects linear-$T$-dependent resistivity to superconducting superfluid density at zero temperature in strongly correlated superconductors. Our analysis suggests that the quantum diffusion might be the origin of this scaling relation. In this case, the charge transport is viewed as a diffusion process of quasi-particles with a diffusion coefficient that approaches the quantum limit, $D \sim \hbar/m^*$.

Method

The high quality $CeCoIn_5$ single crystal samples are grown by an indium self-flux method[6]. High quality crystals were chosen to perform the transport measurements. Four leads were attached to the single crystal, with the current applied parallel to the crystallographic *a* axis. The resistivity was measured both in ambient pressure as well as under hydrostatic pressure *P*.

References

1. Kovtun, P. K., Son, D. T. & Starinets, A. O. Viscosity in Strongly Interacting Quantum Field Theories from Black Hole Physics. *Phys. Rev. Lett.* **94**, 111601 (2005).
2. Sommer, A., Ku, M., Roati, G. & Zwierlein, M. W. Universal spin transport in a strongly interacting Fermi gas. *Nature* **472**, 201–204 (2011).
3. Bardon, A. *et al*. Transverse demagnetization dynamics of a unitary Fermi gas. *Science* **344**, 722–724 (2014).
4. Gurvitch, M. & Fiory, A. T. Resistivity of $La_{1.825}Sr_{0.175}CuO_4$ and $YBa_2Cu_3O_7$ to 1100 K: absence of saturation and its implications. *Phys. Rev. Lett.* **59**, 1337 (1987).
5. Ioffe, A. & Regel, A. Non-crystalline, amorphous and liquid electronic semiconductors. *Prog. Semicond* **4**, 237–291 (1960).
6. Petrovic, C. *et al*. Heavy-fermion superconductivity in $CeCoIn_5$ at 2.3 K. *J. Phys.: Condens. Matter* **13**, L337 (2001).
7. Paglione, J. *et al*. Nonvanishing energy scales at the quantum critical point of $CeCoIn_5$. *Phys. Rev. Lett.* **97**, 106606 (2006).
8. Bruin, J., Sakai, H., Perry, R. & Mackenzie, A. Similarity of scattering rates in metals showing T-linear resistivity. *Science* **339**, 804–807 (2013).
9. Thompson, J. D. & Fisk, Z. Progress in Heavy-Fermion Superconductivity: Ce115 and Related Materials. *J. Phys. Soc. Jpn.* **81**, 011002 (2012).
10. Hall, D. *et al*. Fermi surface of the heavy-fermion superconductor $CeCoIn_5$: The de Haas–van Alphen effect in the normal state. *Phys. Rev. B* **64**, 212508 (2001).
11. Settai, R. *et al*. Quasi-two-dimensional fermi surfaces and the de Haas-van Alphen oscillation in both the normal and superconducting mixed states of $CeCoIn_5$. *J. Phys.: Condens. Matter* **13**, L627 (2001).
12. Knebel, G. *et al*. High-pressure phase diagrams of $CeCoRh_5$ and $CeCoIn_5$ studied by ac calorimetry. *J. Phys.: Condens. Matter* **16**, 8905 (2004).
13. Zaum, S. *et al*. Towards the Identification of a Quantum Critical Line in the (p, B) Phase Diagram of $CeCoIn_5$ with Thermal-Expansion Measurements. *Phys. Rev. Lett.* **106**, 087003 (2011).
14. Hu, T. *et al*. Strong Magnetic Fluctuations in a Superconducting State of $CeCoIn_5$. *Phys. Rev. Lett.* **108**, 056401 (2012).
15. Stock, C., Broholm, C., Hudis, J., Kang, H. J. & Petrovic, C. Spin Resonance in the *d*-Wave Superconductor $cecoin_5$. *Phys. Rev. Lett.* **100**, 087001 (2008).
16. Xiao, H., Hu, T., Almasan, C., Sayles, T. & Maple, M. Pairing symmetry of $CeCoIn_5$ detected by in-plane torque measurements. *Phys. Rev. B* **78**, 014510 (2008).
17. Zhou, B. B. *et al*. Visualizing nodal heavy fermion superconductivity in $CeCoIn_5$. *Nat. Phys.* **9**, 474–479 (2013).
18. Sidorov, V. A. *et al*. Superconductivity and quantum criticality in $CeCoIn_5$. *Phys. Rev. Lett.* **89**, 157004 (2002).
19. Bianchi, A., Movshovich, R., Vekhter, I., Pagliuso, P. & Sarrao, J. Avoided Antiferromagnetic Order and Quantum Critical Point in $CeCoIn_5$. *Phys. Rev. Lett.* **91**, 257001 (2003).
20. Seo, S. *et al*. Disorder in quantum critical superconductors. *Nat. Phys.* **10**, 120–125 (2014).
21. Park, T. *et al*. Hidden magnetism and quantum criticality in the heavy fermion superconductor $CeRhIn_5$. *Nature* **440**, 65–68 (2006).
22. Watanabe, T., Fujii, T. & Matsuda, A. Anisotropic resistivities of Precisely Oxygen Controlled Single-Crystal $Bi_2Sr_2CaCu_2O_{8+\delta}$: Systematic Study on "Spin Gap" Effect. *Phys. Rev. Lett.* **79**, 2113 (1997).
23. Howald, L. *et al*. Strong Pressure Dependence of the Magnetic Penetration Depth in Single Crystals of the Heavy-Fermion Superconductor $CeCoIn_5$ Studied by Muon Spin Rotation. *Phys. Rev. Lett.* **110**, 017005 (2013).
24. Anukool, W., Barakat, S., Panagopoulos, C. & Cooper, J. Effect of hole doping on the london penetration depth in $Bi_{2.15}Sr_{1.85}CaCu_2O_{8+\delta}$ and $Bi_{2.1}Sr_{1.9}Ca_{0.85}Y_{0.15}Cu_2O_{8+\delta}$. *Phys. Rev. B* **80**, 024516 (2009).
25. Uemura, Y. *et al*. Universal Correlations between T_c and n_s/m^*(Carrier Density over Effective Mass) in High-T_c Cuprate Superconductors. *Phys. Rev. Lett.* **62**, 2317 (1989).
26. Homes, C. *et al*. Coherence, incoherence, and scaling along the c axis of $YBa_2Cu_3O_{6+x}$. *Phys. Rev. B* **71**, 184515 (2005).
27. Homes, C. C. *et al*. A universal scaling relation in high-temperature superconductors. *Nature* **430**, 539–41 (2004).
28. Tinkham, M. *Introduction to Superconductivity*: *Second Edition* (Dover Publications, 2004).
29. Gubin, A. I., Ilin, K. S., Vitusevich, S. A., Siegel, M. & Klein, N. Dependence of magnetic penetration depth on the thickness of superconducting Nb thin films. *Phys. Rev. B* **72**, 064503 (2005).
30. Lemberger, T. R., Hetel, I., Tsukada, A., Naito, M. & Randeria, M. Superconductor-to-metal quantum phase transition in overdoped $La_{2-x}Sr_xCuO_4$. *Phys. Rev. B* **83**, 140507 (2011).

31. Hetel, I., Lemberger, T. R. & Randeria, M. Quantum critical behaviour in the superfluid density of strongly underdoped ultrathin copper oxide films. *Nat. Phys.* **3**, 700–702 (2007).
32. Basov, D. N., Timusk, T., Dabrowski, B. & Jorgensen, J. D. *c* -axis response of $YBa_2Cu_4O_8$: A pseudogap and possibility of Josephson coupling of CuO_2 planes. *Phys. Rev. B* **50**, 3511–3514 (1994).
33. Dordevic, S. V. *et al*. Global trends in the interplane penetration depth of layered superconductors. *Phys. Rev. B* **65**, 134511 (2002).
34. Shibauchi, T. *et al*. Anisotropic penetration depth in $La_{2-x}Sr_xCuO_4$. *Phys. Rev. Lett.* **72**, 2263–2266 (1994).
35. Drude, P. Zur elektronentheorie der metalle. *Annalen der Physik* **306**, 566–613 (1900).
36. Tanner, D. *et al*. Superfluid and normal fluid density in high-tc superconductors. *Physica B: Condensed Matter* **244**, 1–8 (1998).
37. Hildebrandt, A. F. Magnetic field of a rotating superconductor. *Physical Review Letters* **12**, 190 (1964).
38. Sanzari, M. A., Cui, H. & Karwacki, F. London moment for heavy-fermion superconductors. *Applied physics letters* **68**, 3802–3804 (1996).
39. Verheijen, A., Van Ruitenbeek, J., de Bruyn Ouboter, R. & de Jongh, L. Measurement of the london moment in two high-temperature superconductors. *Nature* **345**, 418–419 (1990).
40. Padilla, W. J. *et al*. Constant effective mass across the phase diagram of high-T_c cuprates. *Phys. Rev. B* **72**, 060511 (2005).
41. Bandurin, D. A. *et al*. Negative local resistance caused by viscous electron backflow in graphene. *Science* **351**, 1055–1058 (2016).
42. Crossno, J. *et al*. Observation of the Dirac fluid and the breakdown of the Wiedemann-Franz law in graphene. *Science* **351**, 1058–1061 (2016).
43. Moll, P. J. W., Kushwaha, P., Nandi, N., Schmidt, B. & Mackenzie, A. P. Evidence for hydrodynamic electron flow in $PdCoO_2$. *Science* **351**, 1061–1064 (2016).
44. Einstein, A. uber die von der molekularkinetischen theorie der wrme geforderte bewegung von in ruhenden flussigkeiten suspendierten teilchen. *Annalen der physik* **322**, 549–560 (1905).
45. Hartnoll, S. A. Theory of universal incoherent metallic transport. *Nat. Phys.* **11**, 54–61 (2015).
46. Mendelssohn, K. The frictionless state of aggregation. *Proc. Phys. Soc.* **57**, 371 (1945).
47. Hirsch, J. E. Kinetic energy driven superconductivity and superfluidity. *Mod. Phys. Lett. B* **25**, 2219–2237 (2011).
48. Uemura, Y. *et al*. Basic similarities among cuprate, bismuthate, organic, chevrel-phase, and heavy-fermion superconductors shown by penetration-depth measurements. *Phys. Rev. Lett.* **66**, 2665 (1991).
49. Takenaka, K., Mizuhashi, K., Takagi, H. & Uchida, S. Interplane charge transport in $YBa_2Cu_3O_{7-y}$: Spin-gap effect on in-plane and out-of-plane resistivity. *Phys. Rev. B* **50**, 6534 (1994).
50. Tallon, J. *et al*. In-plane Anisotropy of the Penetration Depth Due to Superconductivity on the Cu-O Chains in $YBa_2Cu_3O_{7-\delta}$, $Y_2Ba_4Cu_7O_{15-\delta}$, and $YBa_2Cu_4O_8$. *Phys. Rev. Lett.* **74**, 1008 (1995).
51. Basov, D. *et al*. In-Plane Anisotropy of the Penetration Depth in $YBa_2Cu_3O_{7-x}$ and $YBa_2Cu_4O_8$ Superconductors. *Phys. Rev. Lett.* **74**, 598 (1995).
52. Ando, Y., Segawa, K., Komiya, S. & Lavrov, A. Electrical resistivity anisotropy from self-organized one dimensionality in high-temperature superconductors. *Phys. Rev. Lett.* **88**, 137005 (2002).
53. Tyler, A. *et al*. High-field study of normal-state magnetotransport in $Tl_2Ba_2CuO_{6+\delta}$. *Phys. Rev. B* **57**, R728 (1998).
54. Puchkov, A., Timusk, T., Doyle, S. & Hermann, A. ab-plane optical properties of $Tl_2Ba_2CuO_{6+\delta}$. *Phys. Rev. B* **51**, 3312 (1995).
55. Schmann, J. *et al*. Experimental test of the interlayer pairing models for high-T_c superconductivity using grazing-incidence infrared reflectometry. *Phys. Rev. B* **55**, 11118 (1997).
56. Tsvetkov, A. *et al*. Global and local measures of the intrinsic josephson coupling in $Tl_2Ba_2CuO_6$ as a test of the interlayer tunnelling model. *Nature* **395**, 360–362 (1998).
57. Moler, K. A., Kirtley, J. R., Hinks, D., Li, T. & Xu, M. Images of interlayer Josephson vortices in $Tl_2Ba_2CuO_{6+\delta}$. *Science* **279**, 1193–1196 (1998).
58. Matsuda, A., Sugita, S. & Watanabe, T. Temperature and doping dependence of the $Bi_{2.1}Sr_{1.9}CaCu_2O_{8+\delta}$ pseudogap and superconducting gap. *Phys. Rev. B* **60**, 1377 (1999).
59. Takahashi, H. *et al*. Investigation of the superconducting gap structure in $SrFe_2(As_{0.7}P_{0.3})_2$ by magnetic penetration depth and flux flow resistivity analysis. *Phys. Rev. B* **86**, 144525 (2012).
60. Kasahara, S. *et al*. Evolution from non-Fermi-to fermi-liquid transport via isovalent doping in $BaFe_2(As_{1-x}P_x)_2$ superconductors. *Phys. Rev. B* **81**, 184519 (2010).
61. Hashimoto, K. *et al*. A sharp peak of the zero-temperature penetration depth at optimal composition in $BaFe_2(As_{1-x}P_x)_2$. *Science* **336**, 1554–1557 (2012).
62. Okada, T. *et al*. Magnetic penetration depth and flux-flow resistivity measurements on $NaFe_{0.97}Co_{0.03}As$ single crystals. *Physica C: Superconductivity* **494**, 109–112 (2013).
63. Abdel-Hafiez, M. *et al*. Temperature dependence of lower critical field $H_{c1}(T)$ shows nodeless superconductivity in FeSe. *Phys. Rev. B* **88**, 174512 (2013).
64. Hsu, F.-C. *et al*. Superconductivity in the PbO-type structure α-FeSe. *Proc. Natl. Acad. Sci.* **105**, 14262–14264 (2008).
65. Nakamura, Y. & Uchida, S. Anisotropic transport properties of single-crystal $La_{2-x}Sr_xCuO_4$: Evidence for the dimensional crossover. *Phys. Rev. B* **47**, 8369 (1993).
66. Panagopoulos, C. *et al*. Superfluid response in monolayer high-T_c cuprates. *Phys. Rev. B* **67**, 220502 (2003).
67. Hussey, N. *et al*. Dichotomy in the t-linear resistivity in hole-doped cuprates. *Philos. Trans. R. Soc. London A Math. Phys. Eng. Sci.* **369**, 1626–1639 (2011).
68. Ando, Y., Komiya, S., Segawa, K., Ono, S. & Kurita, Y. Electronic phase diagram of high-T_c cuprate superconductors from a mapping of the in-plane resistivity curvature. *Phys. Rev. Lett.* **93**, 267001 (2004).
69. Russo, P. *et al*. Muon spin relaxation study of superconducting $Bi_2Sr_{2-x}La_xCuO_{6+\delta}$. *Phys. Rev. B* **75**, 054511 (2007).
70. Joynt, R. & Taillefer, L. The superconducting phases of UPt_3. *Rev. Mod. Phys.* **74**, 235 (2002).

Acknowledgements

We sincerely thank Prof. Mianheng Jiang, Prof. Xiaoming Xie, Dr. Wei Li, Prof. Haicang Ren, Prof. Ting-Kuo Lee, Prof. Yan Chen and Prof. Ang Li for discussions. This study was supported by the National Natural Science Foundation of China (Grant Nos 11574338, U1530402, 11522435), the Strategic Priority Research Program (B) of the Chinese Academy of Sciences (Grant Nos XDB04040300, XDB07020200) and the Youth Innovation Promotion Association of the Chinese Academy of Sciences.

Author Contributions

T.H. Planned the research. Y.L. carried out the experiment. T.H. and H.X. wrote the manuscript. G.M. and Y.Y. give fruitful discussions. All authors were intensively involved in the research.

Additional Information

Competing Interests: The authors declare that they have no competing interests.